Journal of Statistical Mechanics:
Theory and Experiment

STOCHASTIC THERMODYNAMICS

Hysteretic thermodynamic uncertainty relation for systems with broken time-reversal symmetry

Journal of Statistical Mechanics: Theory and Experiment
An IOP and SISSA journal

Hysteretic thermodynamic uncertainty relation for systems with broken time-reversal symmetry

Karel Proesmans[1] **and Jordan M Horowitz**[2,3]

[1] Hasselt University, B-3590 Diepenbeek, Diepenbeek, Belgium
[2] Department of Biophysics, University of Michigan, Ann Arbor, MI 48109, United States of America
[3] Center for the Study of Complex Systems, University of Michigan, Ann Arbor, MI 48104, United States of America
E-mail: Karel.Proesmans@uhasselt.be

Received 25 February 2019
Accepted for publication 26 March 2019
Published 24 May 2019

Online at stacks.iop.org/JSTAT/2019/054005
https://doi.org/10.1088/1742-5468/ab14da

Abstract. The thermodynamic uncertainty relation bounds the amount current fluctuations can be suppressed in terms of the dissipation in a mesoscopic system. By considering the fluctuations in the hysteresis of the current—the sum of the currents in the time-forward and time-reversed processes—we extend this relation to systems with broken time-reversal symmetry, either due to the presence of odd state variables, odd driving fields or due to explicit time-dependent driving that is time-reversal asymmetric. We illustrate our predictions on a dilute, weakly-interacting gas driven out of equilibrium by the slow compression of a piston and on a ballistic multi-terminal conductor with an external magnetic field.

Keywords: stochastic thermodynamics

J. Stat. Mech. (2019) 054005

1742-5468/19/054005+17$33.00

Contents

1. Introduction **2**

2. Setup **4**
2.1. Dynamics and environmental entropy flow 4
2.2. Level 2 large deviations for independent trajectories....5

3. Main Result **6**
3.1. Fluctuations of hysteretic currents 6
3.2. Uncertainty bound for hysteretic currents....7

4. Applications **8**
4.1. Isothermal work fluctuations 9
4.2. Steady-state fluctuations within linear response....9

5. Illustrations **10**
5.1. Isothermal work protocol....11
5.2. Multi-terminal conductor....12

6. Conclusion **13**

Acknowledgment **14**

Appendix. Thermodynamic uncertainty relation near equilibrium **15**

References **16**

1. Introduction

In fluctuating systems, stochastic thermodynamics has emerged as a systematic theoretical framework for identifying the thermodynamic properties of currents—such as heat, particle transport and work [1, 2]. Of particular interest is identifying universal energetic trade-offs (or constraints) to such flows, as they often imply general performance bounds on mesoscopic devices [3–7]. One such result is the thermodynamic uncertainty relation, which bounds the fluctuations in the accumulation of a generic current J_T in time T with the system's entropy production rate σ. In its original formulation it states that for a system with Markovian dynamics the relative fluctuations—given as the ratio of the average steady-state flux $\langle j\rangle = \lim_{T\to\infty}\langle J_T\rangle/T$ and variance $\mathrm{Var}(j) = \lim_{T\to\infty}\mathrm{Var}(J_T)/T$—is bounded as [8, 9],

$$\frac{\langle j\rangle^2}{\mathrm{Var}(j)} \leqslant \frac{\sigma}{2k_\mathrm{B}}, \tag{1}$$

where k_B is Boltzmann's constant. This prediction is based on two necessary assumptions: (i) the system relaxes to a unique time-independent steady state, and (ii) the

J. Stat. Mech. (2019) 054005

dynamics are time-reversal symmetric, i.e. the system's configurations and all the forces are even and do not change sign under time reversal, which forbids the presence of, say, magnetic fields. Under these conditions, several extensions have been formulated over the last few years, leading to thermodynamic uncertainty relations for finite-time processes [10–12], equilibrium systems [13], non-Markovian systems [14], and formulations in terms of other variables [15–18]. Furthermore, the above relation has found applications in the study of chemical reaction networks [19–21], molecular motors [22–25], heat engines [26–28], self-assembly [29], synchronization [30], and inference of entropy production [31, 32]. It has also been related to information-theoretic measures [33, 34] and was an inspiration for a new measurement method for diffusion coefficients [35].

If we relax the steady-state assumption and allow time-dependent driving, it is known that the standard thermodynamic uncertainty relation, equation (1), fails [36–45]. However, if one focuses on time-symmetric, periodic driving, say with period Δt, then one can show a weaker bound in the periodic steady state [38],

$$\frac{\langle j_{\Delta t}\rangle^2}{\mathrm{Var}(j_{\Delta t})} \leqslant \frac{1}{2\Delta t}\left(\exp\left(\frac{\Delta S}{k_{\mathrm{B}}}\right)-1\right) \tag{2}$$

where ΔS is the total entropy production over one period with $\langle j_{\Delta t}\rangle = \lim_{n\to\infty}\langle J_{n\Delta t}\rangle/n$ and $\mathrm{Var}(j_{\Delta t}) = \lim_{n\to\infty}\mathrm{Var}(J_{n\Delta t})/n$ the average current and variance per period obtained in the limit that the number of periods n tends to infinity. This relation also holds for discrete-time steady-state Markov chains, where ΔS is the average entropy production per step and Δt its duration. Several alternatives have been proposed for the case where the driving is not time-reversal symmetric [40, 42, 43]. These alternatives rely on the introduction of new quantities that mix thermodynamic with kinematic properties. As a result, the interpretation of their physical meanings can be less transparent than entropy production.

Similar problems arise for steady-state systems with broken time-reversal symmetry, either due to the presence of odd variables or odd external fields. This problem can already be seen in the linear response regime in the presence of a magnetic field, where equation (1) no longer holds due to the breakdown of Onsager symmetry [46]. With odd variables, like the momentum in underdamped Brownian motion, the issues are more subtle as one usually encounters a reversible Hamiltonian evolution perturbed by thermal fluctuations. Thus, currents can flow in phase space even in the absence of dissipation making the validity of equation (1) suspect. The result is that the thermodynamic uncertainty relation cannot be adapted straightforwardly to underdamped dynamics [47–49]. Furthermore, quantum tests of the thermodynamic uncertainty relation that naturally combine Hamiltonian evolution with dissipative dynamics have violated equation (1) [50–52] or required modification and weakening [53, 54].

In this article, we develop a modified thermodynamic uncertainty relation that overcomes some of these difficulties by taking into account the fluctuations in the current of the time-reversed dynamics $\tilde{J}_T$. In particular, we find that the fluctuations in the sum of the current and its time reversal or *hysteretic* current $J_T + \tilde{J}_T$ satisfies a bound of the form

J. Stat. Mech. (2019) 054005

$$\frac{\langle J_T + \tilde{J}_T\rangle^2}{\mathrm{Var}(J_T) + \mathrm{Var}(\tilde{J}_T)} \leqslant \exp\left(\frac{\mathcal{R} + \tilde{\mathcal{R}}}{2}\right) - 1, \tag{3}$$

where $\mathcal{R}$ and $\tilde{\mathcal{R}}$ are particular path averages of the stochastic process and its time-reverse, related to the entropy flow into the environment. We further find particularly transparent interpretations upon specializing to isothermal driven processes or non-equilibrium steady-states within linear response.

2. Setup

Our analysis applies to mesoscopic systems that can be modeled as Markov processes. In this section, we set the stage by reviewing the relevant properties of their dynamics and thermodynamics, before introducing our main theoretical tool, level 2 large deviations for independent trajectories.

2.1. Dynamics and environmental entropy flow

We have in mind a mesoscopic system with configurations labeled by the vector of state variables $\mathbf{x} = \{x_1, \ldots, x_M\}$ whose evolution is driven by a collection of controllable external parameters or forces $\boldsymbol{\lambda} = \{\lambda_1, \ldots, \lambda_\Theta\}$. Both the state variables and control parameters are further assumed to have a well defined symmetry under time-reversal, which we indicate as $\boldsymbol{\epsilon}\mathbf{x} = \{\epsilon_1 x_1, \ldots, \epsilon_M x_M\}$ and $\boldsymbol{\epsilon}\boldsymbol{\lambda} = \{\epsilon_1\lambda_1, \ldots, \epsilon_\Theta\lambda_\Theta\}$ with $\epsilon_i = 1$ for even variables/parameters, such as positions, and $\epsilon_i = -1$ for odd variables/parameters, such as velocities or magnetic fields.

Due to thermal fluctuations, the evolution of the system is stochastic. Thus, in each realization of the process over a time interval $t \in [0, T]$ the system traces out a random trajectory $\Gamma = \{\mathbf{x}(t)\}_{t=0}^{T}$, which we allow to also depend on a specified driving protocol for the parameters $\boldsymbol{\lambda}(t)$. We concisely denote the probability for this trajectory as

$$p_\Gamma = P[\Gamma|\mathbf{x}(0); \boldsymbol{\lambda}(t)]\rho_0[\mathbf{x}(0)] \tag{4}$$

in terms of an initial probability density ρ_0 and the conditional probability P to observe the trajectory under the driving protocol given the initial configuration.

Conjugate to this forward process is a *reverse* process characterized by a time-reversed driving protocol $\tilde{\boldsymbol{\lambda}}(t) = \boldsymbol{\epsilon}\boldsymbol{\lambda}(T - t)$. Allowing for arbitrary initial probability distribution $\tilde{\rho}_0$, we have for the reverse trajectory probability

$$\tilde{p}_\Gamma = P[\Gamma|\mathbf{x}(0); \tilde{\boldsymbol{\lambda}}(t)]\tilde{\rho}_0[\mathbf{x}(0)], \tag{5}$$

where the tilde on $\tilde{p}_\Gamma$ emphasizes that this is a distinct probability on all trajectories Γ characterized by the time-reversed driving $\tilde{\boldsymbol{\lambda}}(t)$.

Having introduced the trajectory probability for the forward process and the reverse process, we can now lean on the theoretical framework of stochastic thermodynamics [1] to connect these trajectory dynamics to thermodynamics. We assume that our dynamics satisfy the principle of local detailed balance, which allows us to identify the entropy flow into the environment with the time-reversal asymmetry of the trajectory

J. Stat. Mech. (2019) 054005

probabilities. In particular, the entropy flow can be identified by comparing the probability of a trajectory Γ in the original forward process to the time-reversed trajectory $\tilde{\Gamma} = \{\boldsymbol{\epsilon}\mathbf{x}(T-t)\}_{t=0}^{T}$ in the reverse process with time-reversed driving [1]:

$$\Delta S_{\rm env} = k_{\rm B} \left\langle \ln \frac{P[\Gamma|\mathbf{x}(0);\boldsymbol{\lambda}(t)]}{P[\tilde{\Gamma}|\boldsymbol{\epsilon}\mathbf{x}(T);\tilde{\boldsymbol{\lambda}}(t)]} \right\rangle_{\boldsymbol{\lambda}(t)}, \tag{6}$$

where the average is over the forward driving. Once we specify the thermodynamic reservoirs in the environment, the entropy flow can be related to the flow of energy through the system. For example, if the environment is composed of a single thermal reservoir at inverse temperature β, then the entropy flow is simply proportional to the heat Q exhausted by the system: $\Delta S_{\rm env} = \beta Q$.

The identification of the environmental entropy flow in the presence of odd variables from the time-reversal asymmetry of the path probability as in equation (6) requires some comment. Microscopic reversibility is not sufficient to make the identification in equation (6) when there are odd-parity variables [55]. However, it has been pointed out that if the environment is composed of thermodynamic reservoirs, then additional symmetries, such as rotational symmetry or spatial parity, allow one to correctly identify the environmental entropy change through the time-reversal asymmetry of the trajectory probability [56–58]. Throughout this paper we will assume such an identification to be possible.

2.2. Level 2 large deviations for independent trajectories

Our main approach to obtaining the inequality in equation (3) will be to analyze the large deviations in the trajectory fluctuations. In this section, we provide a heuristic argument underpinning this approach and review relevant formulas. One could cast the following argument into a more rigorous formulation via a limiting procedure, as was done in [42].

Let us imagine that we take $N \gg 1$ copies of our system, each initialized in ρ_0 and let to evolve independently for a time T under the same driving protocol $\boldsymbol{\lambda}(t)$. Each copy will trace out a different trajectory Γ_i, with $i = 1, \ldots, N$. We can ask what fraction of the copies trace out the same trajectory $q_\Gamma = (1/N)\sum_i \delta(\Gamma - \Gamma_i)$, thereby forming an empirical (or observved) trajectory density. Since each copy is independent, we have, roughly, for the probability distribution of the empirical density

$$\mathcal{P}_N(\{q_\Gamma\}) = \frac{N!}{\prod_\Gamma (N q_\Gamma)!} \left(p_\Gamma\right)^{N q_\Gamma} \sim \mathrm{e}^{-N\mathcal{J}(\{q_\gamma\})}, \tag{7}$$

where we have identified the large deviation rate function from the exponential decay of rare fluctuations [59]

$$\mathcal{J}(\{q_\Gamma\}) = -\lim_{N\to\infty} \frac{1}{N} \ln \mathcal{P}_N(\{q_\Gamma\}) = \sum_\Gamma q_\Gamma \ln\left(\frac{q_\Gamma}{p_\Gamma}\right) \tag{8}$$

as the relative entropy or Kullback–Leibler divergence of the path weights [60]. The argument here, while not formal, is much in the spirit of Sanov's theorem for the empirical density of independent random variables [59].

J. Stat. Mech. (2019) 054005

Ultimately, we are interested in odd currents J_T, which can be expressed as trajectory averages

$$J_T = \sum_{\Gamma} \mathcal{F}_\Gamma q_\Gamma, \tag{9}$$

whose odd-parity under time-reversal is captured by the symmetry with the time-reversed weight $\tilde{\mathcal{F}}_\Gamma$:

$$\mathcal{F}_\Gamma = -\tilde{\mathcal{F}}_{\tilde{\Gamma}}. \tag{10}$$

Fluctuations in J_T can now readily be obtained from our level 2 large deviation function for independent trajectories through the contraction principle [59]

$$\mathcal{I}(J_T) = \min_{\{q_\Gamma\}} \mathcal{J}(\{q_\Gamma\}), \tag{11}$$

where the minimization is over distributions q_Γ that satisfy normalization $\sum_\Gamma q_\Gamma = 1$ and give the correct flux $\sum_\Gamma \mathcal{F}_\Gamma q_\Gamma = J_T$. From this large deviation function, many important properties of the current fluctuations can be deduced. For our purposes, the mean (most likely) current $\langle J_T \rangle$ is the minimum of the large deviation function, which by convention is set to zero: $\mathcal{I}(\langle J_T \rangle) = \mathcal{I}'(\langle J_T \rangle) = 0$. Furthermore, the current variance is obtained from the curvature at the minimum [59]

$$\mathcal{I}''(\langle J_T \rangle) = \frac{1}{\mathrm{Var}(J_T)}. \tag{12}$$

Exactly the same considerations hold for the large deviations of the reverse process with its empirical density $\tilde{q}_\Gamma$ and reverse currents $\tilde{J}_T = \sum_\Gamma \tilde{\mathcal{F}}_\Gamma \tilde{q}_\Gamma$.

3. Main Result

3.1. Fluctuations of hysteretic currents

Our main inequality is a bound on the joint fluctuations of the hysteretic currents, which we address by considering the joint fluctuations of the forward and reverse processes.

Now the fluctuations in the forward process and the reverse process are independent. As such, the joint probability for the empirical density q_Γ and the empirical density for the reverse process $\tilde{q}_\Gamma$ factorizes $\mathcal{P}_N(\{q_\Gamma\}, \{\tilde{q}_{\Gamma'}\}) = \mathcal{P}_N(\{q_\Gamma\})\tilde{\mathcal{P}}_N(\{\tilde{q}_{\Gamma'}\})$. As such, the joint large deviation rate function

$$-\lim_{N\to\infty} \frac{1}{N} \ln \mathcal{P}_N(\{q_\Gamma\}, \{\tilde{q}_{\Gamma'}\}) = \mathcal{J}(\{q_\Gamma\}) + \tilde{\mathcal{J}}(\{\tilde{q}_{\Gamma'}\}) \tag{13}$$

is simply the sum of the large deviation functions of the original process $\mathcal{J}$ and the reverse process $\tilde{\mathcal{J}}$. With this large deviation function we can extract the fluctuations of the hysteretic currents,

$$J_T + \tilde{J}_T = \sum_{\Gamma} \mathcal{F}_\Gamma q_\Gamma + \sum_{\Gamma'} \tilde{\mathcal{F}}_{\Gamma'} \tilde{q}_{\Gamma'}, \tag{14}$$

J. Stat. Mech. (2019) 054005

from the contraction principle

$$\mathcal{I}(J_T + \tilde{J}_T) = \min_{\{q_\Gamma, \tilde{q}_{\Gamma'}\}} \left[\mathcal{J}(\{q_\Gamma\}) + \tilde{\mathcal{J}}(\{\tilde{q}_{\Gamma'}\})\right], \tag{15}$$

where minimization is constrained by

$$\sum_\Gamma q_\Gamma = \sum_{\Gamma'} \tilde{q}_{\Gamma'} = 1, \qquad \sum_\Gamma \mathcal{F}_\Gamma q_\Gamma + \sum_{\Gamma'} \tilde{\mathcal{F}}_{\Gamma'} \tilde{q}_{\Gamma'} = J_T + \tilde{J}_T. \tag{16}$$

3.2. Uncertainty bound for hysteretic currents

While the minimization in equation (15) can rarely be done analytically, a useful upper bound can be found using the variational ansatz—which is a slight variation of the ansatz used in [38] to obtain equation (2)—

$$\begin{aligned} q_\Gamma^{(J_T+\tilde{J}_T)} &= p_\Gamma + \frac{J_T + \tilde{J}_T - \left\langle J_T + \tilde{J}_T \right\rangle}{\left\langle J_T + \tilde{J}_T \right\rangle} \left(p_\Gamma - \frac{p_\Gamma \tilde{p}_{\tilde{\Gamma}}}{\mathcal{N}\,(p_\Gamma + \tilde{p}_{\tilde{\Gamma}})} \right) \\ \tilde{q}_\Gamma^{(J_T+\tilde{J}_T)} &= \tilde{p}_\Gamma + \frac{J_T + \tilde{J}_T - \left\langle J_T + \tilde{J}_T \right\rangle}{\left\langle J_T + \tilde{J}_T \right\rangle} \left(\tilde{p}_\Gamma - \frac{p_{\tilde{\Gamma}} \tilde{p}_\Gamma}{\mathcal{N}\,(p_{\tilde{\Gamma}} + \tilde{p}_\Gamma)} \right), \end{aligned} \tag{17}$$

with

$$\mathcal{N} = \sum_\Gamma \frac{p_\Gamma \tilde{p}_{\tilde{\Gamma}}}{p_\Gamma + \tilde{p}_{\tilde{\Gamma}}}, \tag{18}$$

where we emphasize that $\tilde{p}_{\tilde{\Gamma}}$ is the probability in the reverse process to observe $\tilde{\Gamma}$, the time reverse of the trajectory Γ. The rationale for this ansatz can be seen by recognizing it as an expansion of q_Γ around its most likely value p_Γ to first order in the deviation in the hysteric current around its typical value, while maintaining the constraints. While many ansatzs could satisfy this criteria, this one minimizes the resulting bound on the variance.

Using equation (10), it is clear that the conditions in equation (16) are valid, and therefore,

$$\mathcal{I}(J_T + \tilde{J}_T) \leqslant \mathcal{J}(\{q_\Gamma^{(J_T+\tilde{J}_T)}\}) + \tilde{\mathcal{J}}(\{\tilde{q}_\Gamma^{(J_T+\tilde{J}_T)}\}). \tag{19}$$

This translates into a bound on variance through equation (12) after noting that $\mathcal{J}(\{q_\Gamma^{(\langle J_T+\tilde{J}_T\rangle)}\}) = \mathcal{J}'(\{q_\Gamma^{(\langle J_T+\tilde{J}_T\rangle)}\}) = 0$ (and analogous relations for $\tilde{\mathcal{J}}$),

$$\mathcal{I}''(\langle J_T + \tilde{J}_T\rangle) = \frac{1}{\mathrm{Var}(J_T + \tilde{J}_T)} \leqslant \frac{1}{\left\langle J_T + \tilde{J}_T \right\rangle^2} \left(\frac{1}{\mathcal{N}} - 2 \right). \tag{20}$$

To arrive at the final result, we now need to bound $\mathcal{N}$. Following closely [38], we introduce the pair of trajectory averages with an eye towards entropy flow (see equation (6)),

J. Stat. Mech. (2019) 054005

$$\mathcal{R}+\tilde{\mathcal{R}}=\sum_{\Gamma}p_{\Gamma}\ln\frac{p_{\Gamma}}{\tilde{p}_{\tilde{\Gamma}}}+\sum_{\Gamma'}\tilde{p}_{\Gamma'}\ln\frac{\tilde{p}_{\Gamma'}}{p_{\tilde{\Gamma}'}}. \tag{21}$$

Now from the definition of $\mathcal{N}$ (equation (18)) and an application of Jensen's inequality we have

$$\begin{aligned}\ln\mathcal{N}+\frac{\mathcal{R}+\tilde{\mathcal{R}}}{2}&=\ln\left(\sum_{\Gamma}\frac{p_{\Gamma}\tilde{p}_{\tilde{\Gamma}}}{p_{\Gamma}+\tilde{p}_{\tilde{\Gamma}}}\right)+\sum_{\Gamma}\frac{p_{\Gamma}-\tilde{p}_{\tilde{\Gamma}}}{2}\ln\left(\frac{p_{\Gamma}}{\tilde{p}_{\tilde{\Gamma}}}\right)\\&\geqslant\sum_{\Gamma}\frac{p_{\Gamma}+\tilde{p}_{\tilde{\Gamma}}}{2}\ln\left(\frac{2p_{\Gamma}\tilde{p}_{\tilde{\Gamma}}}{(p_{\Gamma}+\tilde{p}_{\tilde{\Gamma}})^2}\right)+\sum_{\Gamma}\frac{p_{\Gamma}-\tilde{p}_{\tilde{\Gamma}}}{2}\ln\left(\frac{p_{\Gamma}}{\tilde{p}_{\tilde{\Gamma}}}\right)\\&=\sum_{\Gamma}\tilde{p}_{\tilde{\Gamma}}\left(\frac{1+u_{\Gamma}}{2}\ln\frac{2u_{\Gamma}}{(1+u_{\Gamma})^2}+\frac{u_{\Gamma}-1}{2}\ln u_{\Gamma}\right),\end{aligned} \tag{22}$$

with $u_{\Gamma}=p_{\Gamma}/\tilde{p}_{\tilde{\Gamma}}$. Using the one-dimensional inequality [38, 42]

$$\frac{1+u}{2}\ln\frac{2u}{(1+u)^2}+\frac{u-1}{2}\ln u\geqslant(1-\ln 2)\frac{1+u}{2}-\frac{2u}{u+1}, \tag{23}$$

which can be verified upon graphical inspection, one can do the summation in the last line of equation (22) explicitly, leading to

$$\ln\mathcal{N}+\frac{\mathcal{R}+\tilde{\mathcal{R}}}{2}\geqslant 1-\ln 2-2\mathcal{N}\geqslant\ln(1-\mathcal{N}), \tag{24}$$

where the last inequality follows from the concavity of the logarithmic function. It now readily follows that

$$\frac{1}{\mathcal{N}}\leqslant \mathrm{e}^{\frac{\mathcal{R}+\tilde{\mathcal{R}}}{2}}+1. \tag{25}$$

Plugging this back in into equation (20), immediately leads to the final result in equation (3), after noting that since the two processes are independent the joint variance is the sum of the individual variances.

4. Applications

The path averages $\mathcal{R}+\tilde{\mathcal{R}}$ in equation (21) are intimately related to the entropy flow in equation (6). Indeed, we can peel off the entropy flow contribution as follows. For $\mathcal{R}$ (and analogously for $\tilde{\mathcal{R}}$), we have

$$\mathcal{R}=\Delta S_{\mathrm{env}}/k_{\mathrm{B}}+\mathcal{B} \tag{26}$$

where we have singled out the boundary contribution

$$\mathcal{B}=\left\langle\ln\frac{\rho_0(\mathbf{x}(0))}{\tilde{\rho}_0(\boldsymbol{\epsilon}\mathbf{x}(T))}\right\rangle_{\boldsymbol{\lambda}(t)}=\sum_{\mathbf{x}}\rho_0(\mathbf{x})\ln\rho_0(\mathbf{x})-\sum_{\mathbf{x}}\rho_T(\mathbf{x})\ln\tilde{\rho}_0(\boldsymbol{\epsilon}\mathbf{x}), \tag{27}$$

J. Stat. Mech. (2019) 054005

with ρ_T the final distribution of the forward process. Roughly speaking, this boundary contribution $\mathcal{B}$ quantifies the time-reversal asymmetry between the initial and terminal distributions of the two processes. Though to provide $\mathcal{B}$ with a clear thermodynamic interpretation, we need to specify these distributions. In this section, we explore some possible choices.

4.1. Isothermal work fluctuations

Let us specialize to systems coupled to a single thermal reservoir at inverse temperature β. In the absence of driving, we assume the system relaxes to a thermal equilibrium state given by the Botlzmann distribution $\rho^{\mathrm{eq}}(\mathbf{x};\boldsymbol{\lambda}) = \mathrm{e}^{\beta(F(\boldsymbol{\lambda})-E(\mathbf{x};\boldsymbol{\lambda}))}$ with time-reversal invariant energy function $E(\mathbf{x};\boldsymbol{\lambda}) = E(\boldsymbol{\epsilon}\mathbf{x};\boldsymbol{\epsilon}\boldsymbol{\lambda})$ and free energy $F(\boldsymbol{\lambda})$.

An interesting choice for initial conditions in this situation is to choose the initial distribution of the forward process to be the initial equilibrium distribution $\rho_0(\mathbf{x}) = \rho^{\mathrm{eq}}(\mathbf{x};\boldsymbol{\lambda}(0))$ and for the reverse process the final equilibrium distribution $\tilde{\rho}_0(\mathbf{x}) = \rho^{\mathrm{eq}}(\mathbf{x};\boldsymbol{\lambda}(T))$ [61]. In this case,

$$\mathcal{R} + \tilde{\mathcal{R}} = \beta\langle W_T + \tilde{W}_T\rangle, \tag{28}$$

is simply the sum of the work into the system in the forward and reverse processes, i.e. the work hysteresis [62, 63].

A particular interesting current is then the work hysteresis itself, $W_T + \tilde{W}_T$, leading to the thermodynamic bound on work fluctuations

$$\frac{\left\langle W_T + \tilde{W}_T \right\rangle^2}{\mathrm{Var}(W_T) + \mathrm{Var}(\tilde{W}_T)} \leqslant \exp\left(\frac{\beta}{2}\langle W_T + \tilde{W}_T\rangle\right) - 1. \tag{29}$$

It should be noted that this bound on work fluctuations is independent of the work fluctuation relations [61], offering an orthogonal constraint to the structure of work distributions.

4.2. Steady-state fluctuations within linear response

Another special case where progress can be made is systems at near-equilibrium steady states. Let us assume that when the parameters are time-independent $\boldsymbol{\lambda}$, the system relaxes to a parameter-dependent steady-state distribution $\pi(\mathbf{x};\boldsymbol{\lambda})$. By choosing the initial distribution of the forward process as the steady-state distribution $\rho_0(\mathbf{x}) = \pi(\mathbf{x};\boldsymbol{\lambda})$ and initiating the reverse process in the parameter-reversed steady-state distribution $\tilde{\rho}_0(\mathbf{x}) = \pi(\mathbf{x};\boldsymbol{\epsilon}\boldsymbol{\lambda})$ we find that the boundary contributions sum to

$$\mathcal{B} + \tilde{\mathcal{B}} = \sum_{\mathbf{x}} \pi(\mathbf{x};\boldsymbol{\lambda}) \ln \frac{\pi(\mathbf{x};\boldsymbol{\lambda})}{\pi(\boldsymbol{\epsilon}\mathbf{x};\boldsymbol{\epsilon}\boldsymbol{\lambda})} + \sum_{\mathbf{x}} \pi(\mathbf{x};\boldsymbol{\epsilon}\boldsymbol{\lambda}) \ln \frac{\pi(\mathbf{x};\boldsymbol{\epsilon}\boldsymbol{\lambda})}{\pi(\boldsymbol{\epsilon}\mathbf{x};\boldsymbol{\lambda})}, \tag{30}$$

which is a symmetrized relative entropy (Jensen–Shannon divergence [60]) of the steady-state distribution with its time reverse. Thus, when the steady-state distribution is time-reversal symmetric these boundary terms drop out. This term has previously been identified in [55, 64] as an unavoidable component in the analysis of the thermodynamics of systems with broken time-reversal symmetry.

J. Stat. Mech. (2019) 054005

It is now very natural, in light of the original thermodynamic uncertainty relation in equation (1), to consider how our bound constrains the long time limit of the current fluctuations: $\langle J_T\rangle = T\langle\, j\rangle$ and $\mathrm{Var}(J_T) \to T\,\mathrm{Var}(\,j)$. Unfortunately, our result turns out not to be informative in this limit: for long times the entropy flow grows linearly with time $\Delta S_{\mathrm{env}} = T\sigma$ causing the our upper bound to diverge. Thus, despite the close formal similarity with previous results, direct comparison is challenging. Interesting progress can be made however for systems near equilibrium within linear response.

Within linear response all currents and conjugate thermodynamic forces are small, but their fluctuations need not be. To formalize this notion, it is helpful to introduce a small parameter η that 'measures' the distance from equilibrium; roughly, the strength of the thermodynamic forces holding the system slightly out of equilibrium. As the entropy flow is a bilinear function of currents and forces, it too is small but behaves as $\sim \eta^2$. Similarly, one can show using standard perturbation theory that if the steady-state is near equilibrium as assumed, $\pi(\mathbf{x};\boldsymbol{\lambda}) = \rho^{\mathrm{eq}}(\mathbf{x},\boldsymbol{\lambda}) + \eta\ \delta\pi(\mathbf{x};\boldsymbol{\lambda})$, then the boundary terms as relative entropies also behave as $\sim \eta^2$. Thus, we can make a consistent expansion of our uncertainty relation in equation (3) utilizing our identifications in equations (26) and (27) resulting in the near-equilibrium bound

$$\frac{\langle J_T + \tilde{J}_T\rangle^2}{\mathrm{Var}(J_T) + \mathrm{Var}(\tilde{J}_T)} \leqslant \frac{\Delta S_{\mathrm{env}} + \Delta\tilde{S}_{\mathrm{env}}}{2k_{\mathrm{B}}} + \frac{\delta\mathcal{B} + \delta\tilde{\mathcal{B}}}{2}, \tag{31}$$

with $\delta\mathcal{B}$ and $\delta\tilde{\mathcal{B}}$ the lowest-order linear-response corrections to the boundary terms, which are zero for time-reversal symmetric steady-states.

Interestingly, the steady-state version of this linear response inequality is reminiscent of the original formulation of the uncertainty relation. Indeed, returning to the steady-state current $\langle\, j\rangle = \lim_{T\to\infty}\langle J_T\rangle/T$, variance $\mathrm{Var}(\,j) = \lim_{T\to\infty}\mathrm{Var}(J_T)/T$, and entropy flow which becomes equal to the entropy production rate in the steady state $\sigma = \lim_{T\to\infty}\Delta S_{\mathrm{env}}/T$, we have

$$\frac{\left\langle\, j + \tilde{j}\right\rangle^2}{\mathrm{Var}(\,j) + \mathrm{Var}\left(\tilde{j}\right)} \leqslant \frac{\sigma + \tilde{\sigma}}{2k_{\mathrm{B}}}, \tag{32}$$

after noting that the boundary terms are not extensive in time. In the appendix, we provide an alternative viewpoint on this prediction by deriving it entirely within the framework of linear response theory.

5. Illustrations

In this section, we provide two illustrations that highlight the utility of the two applications discussed in the previous section. The first example is a model for the adiabatic expansion/compression of a dilute, weakly-interacting gas. The second is a steady-state multi-terminal conductor in an external magnetic field within linear response.

https://doi.org/10.1088/1742-5468/ab14da

J. Stat. Mech. (2019) 054005

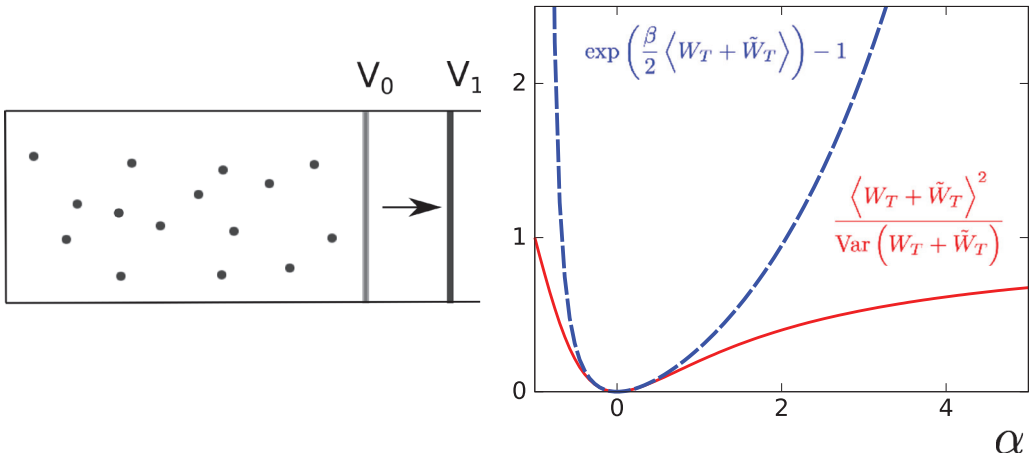

Figure 1. Left panel: depiction of a dilute gas confined to a box with a movable piston used to expand the volume from V_0 to V_1. Right panel: verification of the work uncertainty relation for $d = 2$, $N = 1$ as a function of the work-distribution parameter $\alpha = (V_0/V_1)^{2/d} - 1$.

5.1. Isothermal work protocol

Our first illustration is a solvable model developed by Crooks and Jarzynski [65]. The system of interest is a dilute, weakly-interacting gas of N particles confined to a box in d dimensions with one wall actuated by a movable piston that allows one to do work by varying the volume, figure 1. The gas is initialized in thermal equilibrium at inverse temperature β and volume V_0 by coupling the gas to a large thermal reservoir. The reservoir is then disconnected and the piston is slowly, adiabatically compressed (or expanded) changing the volume from $V_0 \to V_1$.

In this model, the full probability distribution of work can be determined analytically [65], and is given by the Gamma distribution parameterized by $\alpha = (V_0/V_1)^{2/d} - 1$ as

$$P(W) = \frac{\beta}{|\alpha|\Gamma(k)} \left(\frac{\beta W}{\alpha}\right)^{k-1} \mathrm{e}^{-\beta W/\alpha} \theta(\alpha W), \tag{33}$$

with shape parameter $k = dN/2$, where $\Gamma(k)$ is the Gamma function and $\theta(y)$ is the Heaviside step function. For example, a compression has $V_0 > V_1$ implying $\alpha > 0$ and the work distribution is supported only on the positive work values.

We will now consider the forward process to be compression from $V_0 \to V_1$ with associated parameter $\alpha = (V_0/V_1)^{2/d} - 1$, and the reverse process is expansion from $V_1 \to V_0$ with $\tilde{\alpha} = (V_1/V_0)^{2/d} - 1$. Reading off the mean $\langle W_T \rangle = k\alpha/\beta$ and variance $\mathrm{Var}(W_T) = k\alpha^2/\beta^2$ from the Gamma distribution, one can check that the work uncertainty relation, equation (29),

$$\frac{\mathrm{d}N}{2} \frac{(\alpha + \tilde{\alpha})^2}{\alpha^2 + \tilde{\alpha}^2} \leqslant \exp\left(\frac{\mathrm{d}N}{4}(\alpha + \tilde{\alpha})\right) - 1, \tag{34}$$

is valid as $\tilde{\alpha} = (1 + \alpha)^{-1} - 1$. This result is illustrated in figure 1.

J. Stat. Mech. (2019) 054005

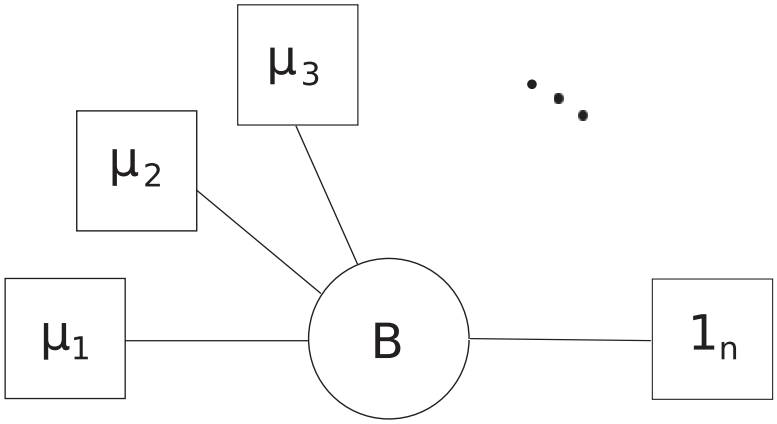

Figure 2. Illustration of a multi-terminal conductor: a central scattering region (circle) in a magnetic field B exchanges particles with n particle reservoirs with chemical potentials $\mu_1, \ldots, \mu_n$ and equal inverse temperature β.

5.2. Multi-terminal conductor

Consider a collection of n particle reservoirs, connected via a central scattering region in a magnetic field B, where each reservoir α has a constant inverse temperature β and chemical potential μ_α, $\alpha = 1, \ldots, n$, see figure 2. This class of systems was studied previously in the context of thermodynamic uncertainty relations in [46], where it was shown that the original uncertainty relation, equation (1), does not hold due to the presence of the magnetic field.

We are interested in the particle flux to each reservoir α. This can be written in terms of the transmission matrix $\mathcal{T}_{\mathbf{B}}^{\alpha\gamma}(E)$, which gives the rate at which a particle starting at reservoir α with energy E ends up in reservoir γ. The flux is then given by the multi-terminal Landauer formula [66–68],

$$\langle j_\alpha \rangle = \frac{1}{h} \int_0^\infty \mathrm{d}E \sum_\gamma \mathcal{T}_{\mathbf{B}}^{\alpha\gamma}(E)(u^\alpha(E) - u^\gamma(E)), \tag{35}$$

where h is Planck's constant and

$$u^\alpha(E) = \exp\left[-\beta(E - \mu_\alpha)\right]. \tag{36}$$

One can show that the variance associated with the particle flux is given by [53]

$$\mathrm{Var}(j_\alpha) = \frac{1}{h} \int_0^\infty \mathrm{d}E \sum_{\gamma \neq \alpha} \mathcal{T}_{\mathbf{B}}^{\alpha\gamma}(E)(u^\alpha(E) + u^\gamma(E)), \tag{37}$$

and the average entropy production rate is

$$\sigma = \sum_\alpha F_\alpha j_\alpha, \tag{38}$$

with

$$F_\alpha = \beta(\mu_\alpha - \mu_0), \tag{39}$$

J. Stat. Mech. (2019) 054005

μ_0 being an arbitrary, constant chemical potential.

In the time-reversed situation, where the magnetic field reverses its sign, the above expressions stay the same apart from the transmission matrix $\tilde{\mathcal{T}}^{\alpha\gamma}_{\mathbf{B}}(E) = \mathcal{T}^{\alpha\gamma}_{-\mathbf{B}}(E)$. The transmission matrix does however satisfy an important Onsager–Casimir-like symmetry relation [68],

$$\mathcal{T}^{\alpha\gamma}_{-\mathbf{B}}(E) = \mathcal{T}^{\gamma\alpha}_{\mathbf{B}}(E). \tag{40}$$

From these basic expressions, formulas for the hysteretic fluctuations follow readily. They are conveniently expressed through the quantities [46]

$$\mathcal{V}^{\alpha\gamma}_{\mathbf{B}} = \frac{1}{h}\int_0^\infty \mathrm{d}E\,\left(\mathcal{T}^{\alpha\gamma}_{\mathbf{B}}(E) + \tilde{\mathcal{T}}^{\alpha\gamma}_{\mathbf{B}}(E)\right) u^\gamma(E), \qquad \mathcal{D}_{\alpha\gamma} = F_\alpha - F_\gamma \tag{41}$$

as

$$\left\langle j_\alpha + \tilde{j}_\alpha \right\rangle = \sum_\gamma \mathcal{V}^{\alpha\gamma}_{\mathbf{B}}\left(\mathrm{e}^{\mathcal{D}_{\alpha\gamma}} - 1\right) \tag{42}$$

$$\mathrm{Var}(j_\alpha) + \mathrm{Var}(\tilde{j}_\alpha) = \sum_{\gamma\neq\alpha} \mathcal{V}^{\alpha\gamma}_{\mathbf{B}}\left(\mathrm{e}^{\mathcal{D}_{\alpha\gamma}} + 1\right) \tag{43}$$

$$\sigma + \tilde{\sigma} = \frac{k_\mathrm{B}}{2}\sum_{\alpha,\gamma} \mathcal{V}^{\alpha\gamma}_{\mathbf{B}}\mathcal{D}_{\alpha\gamma}\left(\mathrm{e}^{\mathcal{D}_{\alpha\gamma}} - 1\right). \tag{44}$$

We can now verify the linear response uncertainty relation in equation (32) by demonstrating that $X = (\sigma+\tilde{\sigma})(\mathrm{Var}(j_\alpha) + \mathrm{Var}(\tilde{j}_\alpha))/(2k_\mathrm{B}) - \left\langle j_\alpha + \tilde{j}_\alpha\right\rangle^2$ is positive. To this end, we first note that $\mathcal{V}^{\alpha\gamma}_{\mathbf{B}}\left(\mathrm{e}^{\mathcal{D}_{\alpha\gamma}} - 1\right) = -\mathcal{V}^{\gamma\alpha}_{\mathbf{B}}\left(\mathrm{e}^{\mathcal{D}_{\gamma\alpha}} - 1\right)$, and therefore

$$\sigma + \tilde{\sigma} \geqslant \frac{k_\mathrm{B}}{h}\sum_{\gamma} \mathcal{V}^{\alpha\gamma}_{\mathbf{B}}\mathcal{D}_{\alpha\gamma}\left(\mathrm{e}^{\mathcal{D}_{\alpha\gamma}} - 1\right). \tag{45}$$

Now combining equations (42)–(45), we find

$$\begin{aligned} X &\geqslant \frac{1}{h}\sum_{\gamma,\gamma'} \mathcal{V}^{\alpha\gamma}_{\mathcal{B}}\mathcal{V}^{\alpha\gamma'}_{\mathcal{B}}\left(\frac{\mathcal{D}_{\alpha\gamma}}{2}\left(\mathrm{e}^{\mathcal{D}_{\alpha\gamma}} - 1\right)\left(\mathrm{e}^{\mathcal{D}_{\alpha\gamma'}} + 1\right) - \left(\mathrm{e}^{\mathcal{D}_{\alpha\gamma}} - 1\right)\left(\mathrm{e}^{\mathcal{D}_{\alpha\gamma'}} - 1\right)\right) \\ &\geqslant \frac{2}{h}\sum_{\gamma,\gamma'} \mathcal{V}^{\alpha\gamma}_{\mathcal{B}}\mathcal{V}^{\alpha\gamma'}_{\mathcal{B}}\frac{\left(\mathrm{e}^{\mathcal{D}_{\alpha\gamma}} - \mathrm{e}^{\mathcal{D}_{\alpha\gamma'}}\right)^2}{(\mathrm{e}^{\mathcal{D}_{\alpha\gamma}} + 1)(\mathrm{e}^{\mathcal{D}_{\alpha\gamma'}} + 1)} \\ &\geqslant 0, \end{aligned} \tag{46}$$

where we used the inequality $y(\exp(y) - 1) \geqslant 2(\exp(y) - 1)^2/(\exp(y) + 1)$.

6. Conclusion

In this paper, we derived a finite-time thermodynamic uncertainty relation for systems with broken time-reversal symmetry by looking at hysteretic currents—joint current

J. Stat. Mech. (2019) 054005

fluctuations in the time-forward and time-reversed processes. Our result implies that for nonequilibrium steady-states within linear response, the original thermodynamic uncertainty relation holds as long as we account for the time-reversal asymmetry of the steady state. When this hysteretic uncertainty relation is specialized to driven isothermal work processes, it implies a nontrivial relationship between the fluctuations of the work in the forward and reverse process. In each case, the quantities have clear physical and thermodynamic interpretations. We have also verified that the hysteretic uncertainty relation holds for two examples that strictly do not fall within our setup: a ballistic multi-terminal conductor as well as for slow, adiabatic compression of a gas. This raises an interesting question as to the generality of our extension, a question which might be answered by doing a fully Hamiltonian derivation of the thermodynamic uncertainty relation.

We have also seen that direct comparison with earlier results for steady-state currents arbitrarily far from equilibrium is challenged by the structure of our bound. A similar difficulty arrises when comparing with uncertainty bounds derived for systems driven by time-periodic protocols, where the issue of taking the limit of number of periods to infinity leads to an uninformative inequality. Indeed, in [40, 42, 43], relations similar to equations (1) and (2) were derived for systems with time-asymmetric driving, but focused on this long-time limit. On the other hand, our finite-time results only depend on the entropy production, while previous results mixed entropy production with various other quantities. Some use measures of the time-reversal symmetry breaking in the kinetics. Others introduce entropy-production-like quantities but utilizing time-averaged current and forces. It would be interesting to see how our bound compares to these results from the literature more precisely.

Beyond the cases considered here one can think of several other classes of systems where the hysteretic uncertainty relation can give new physical insights. One could for example think about systems which are prepared in echo states [69]. Another interesting extension would be to quantum systems, where one might overcome some of the observed deficiencies in the original uncertainty relation [51, 53]. It would also be interesting to see if one can use the hysteretic uncertainty relation to constrain the performance of heat engines with broken time-reversal symmetry, in a similar way as was done for time-symmetric steady-state driving [26].

Acknowledgment

The authors acknowledge the Max Planck Institute for the Physics of Complex Systems which hosted the International Workshop ‘Stochastic Thermodynamics: Experiment and Theory’ where this work was initiated as well as Hugo Touchette for useful remarks. KP is a postdoctoral fellow of the Research Foundation-Flanders (FWO). JMH is supported by the Gordon and Betty Moore Foundation as a Physics of Living Systems Fellow through Grant No. GBMF4513.

J. Stat. Mech. (2019) 054005

Appendix. Thermodynamic uncertainty relation near equilibrium

In this appendix, we give an alternative derivation of the hysteretic thermodynamic uncertainty relation in the linear response regime, presented in section 4.2, using linear response theory [70]. Previous derivations of the time-symmetric uncertainty relation within linear response [8, 46] relied on the Onsager matrix being positive-definite. Similar to these approahes, we will see by using hysteretic currents, that we can again exploit the fact that the symmetric part of the Onsager–Casimir matrix is positive-definite. (In general, the Onsager–Casimir matrix itself is not positive-definite.)

For notational simplicity, we will focus on a system with two independent thermodynamic fluxes J_1 and J_2 with thermodynamic forces F_1 and F_2 conjugated through the entropy production rate $\sigma = k_{\rm B}(J_1F_1 + J_2F_2)$. The following can easily be extended to systems with more thermodynamic fluxes. In the linear response regime, the currents can be expanded linearly in terms of the forces [70]

$$J_1 = L_{11}F_1 + L_{12}F_2, \qquad J_2 = L_{21}F_1 + L_{22}F_2, \tag{A.1}$$

where the expansion parameters L_{ij} are known as the Onsager coefficients. In terms of these coefficients, the entropy production can be written as the quadratic form

$$\sigma = k_{\rm B}\sum_{i,j=1}^{2} F_i L_{ij} F_j. \tag{A.2}$$

Notably, if we introduce the symmetric and antisymmetric Onsager coeffecients

$$L_{ij}^{(s)} = \frac{L_{ij} + L_{ji}}{2}, \qquad L_{ij}^{(a)} = \frac{L_{ij} - L_{ji}}{2}, \tag{A.3}$$

then the entropy production only depends on the symmetrized coeffecients, $\sigma = k_{\rm B}\sum_{i,j=1}^{2} F_i L_{ij}^{(s)} F_j$. The second law then guarantees the positivity of the entropy production independent of the choice of F_i, which implies the useful condition on the symmetric Onsager coefficients

$$L_{11}^{(s)} L_{22}^{(s)} \geqslant {L_{12}^{(s)}}^2. \tag{A.4}$$

Analogously, we can write for the time-reversed dynamics (assuming the thermodynamic forces to be time-reversal symmetric),

$$\tilde{J}_1 = \tilde{L}_{11}F_1 + \tilde{L}_{12}F_2, \qquad \tilde{J}_2 = \tilde{L}_{21}F_1 + \tilde{L}_{22}F_2 \tag{A.5}$$

where the time-reversed Onsager matrix can be related to the time-forward Onsager matrix via Onsager–Casimir symmetry [70],

$$\tilde{L}_{ij} = L_{ji}. \tag{A.6}$$

The Onsager–Casimir symmetry further determines the symmetric and anti-symmetric Onsager coefficients associated with the time-reversed driving

$$\tilde{L}_{ij}^{(s)} = L_{ij}^{(s)}, \qquad \tilde{L}_{ij}^{(a)} = -L_{ij}^{(a)}. \tag{A.7}$$

As such, within linear response the entropy production of time-forward and time-reversed dynamics are equal:

J. Stat. Mech. (2019) 054005

$$\tilde{\sigma} \equiv k_{\mathrm{B}} \sum_{i,j=1}^{2} \tilde{J}_i F_i = k_{\mathrm{B}} \sum_{i,j=1}^{2} F_i \tilde{L}_{ij}^{(s)} F_j = \sigma. \tag{A.8}$$

The Onsager–Casimir symmetry significantly simplifies the quantities appearing in the hysteretic uncertainty relation. Indeed, we have the hysteretic entropy production rate

$$\sigma + \tilde{\sigma} = 2k_{\mathrm{B}} \sum_{i,j} F_i L_{ij}^{(s)} F_j. \tag{A.9}$$

From the definition of the thermodynamic fluxes, equation (A.1), and the above constrains, we can also write

$$\left\langle J_1 + \tilde{J}_1 \right\rangle = 2\left(L_{11}^{(s)} F_1 + L_{12}^{(s)} F_2\right), \tag{A.10}$$

and an analogous relation for J_2. Meanwhile, the variance of the fluxes can be written in terms of the Onsager coefficients via the fluctuation-dissipation relation,

$$\mathrm{Var}(J_1) = 2L_{11}^{(s)}, \tag{A.11}$$

and therefore,

$$\mathrm{Var}(J_1 + \tilde{J}_1) = 4L_{11}^{(s)}. \tag{A.12}$$

Combining these results leads to

$$\begin{aligned} \frac{(\sigma + \tilde{\sigma})\mathrm{Var}(J_1 + \tilde{J}_1)}{2k_{\mathrm{B}}} - \left\langle J_1 + \tilde{J}_1 \right\rangle^2 &= 4L_{11}^{(s)} \sum_{j,k} F_j L_{jk}^{(s)} F_k \\ &\quad - 4 \sum_{k,l} F_k L_{1k}^{(s)} L_{1j}^{(s)} F_j \\ &= 4F_2^2 \left(L_{11}^{(s)} L_{22}^{(s)} - {L_{12}^{(s)}}^2\right) \\ &\geqslant 0, \end{aligned} \tag{A.13}$$

which verifies equation (32).

References

[1] Seifert U 2012 *Rep. Prog. Phys.* **75** 126001
[2] Van den Broeck C and Esposito M 2015 *Physica* A **418** 6–16
[3] Funo K and Ueda M 2015 *Phys. Rev. Lett.* **115** 260601
[4] Brandner K, Saito K and Seifert U 2015 *Phys. Rev.* X **5** 031019
[5] Proesmans K and Van den Broeck C 2015 *Phys. Rev. Lett.* **115** 090601
[6] Proesmans K, Cleuren B and Van den Broeck C 2016 *Phys. Rev. Lett.* **116** 220601
[7] Shiraishi N, Saito K and Tasaki H 2016 *Phys. Rev. Lett.* **117** 190601
[8] Barato A C and Seifert U 2015 *Phys. Rev. Lett.* **114** 158101
[9] Gingrich T R, Horowitz J M, Perunov N and England J L 2016 *Phys. Rev. Lett.* **116** 120601
[10] Pietzonka P, Ritort F and Seifert U 2017 *Phys. Rev.* E **96** 012101
[11] Horowitz J M and Gingrich T R 2017 *Phys. Rev.* E **96** 020103
[12] Dechant A and Sasa S I 2018 *J. Stat. Mech.* 063209
[13] Guioth J and Lacoste D 2016 *Europhys. Lett.* **115** 60007

J. Stat. Mech. (2019) 054005

[14] Knoops G and Vanderzande C 2018 *Phys. Rev.* E **97** 052408
[15] Garrahan J P 2017 *Phys. Rev.* E **95** 032134
[16] Gingrich T R and Horowitz J M 2017 *Phys. Rev. Lett.* **119** 170601
[17] Nardini C and Touchette H 2018 *Eur. Phys. J.* B **91** 16
[18] Di Terlizzi I and Baiesi M 2018 *J. Phys. A: Math. Theor.* **52** 02LT03
[19] Barato A C and Seifert U 2015 *J. Phys. Chem.* B **119** 6555–61
[20] Pietzonka P, Barato A C and Seifert U 2016 *J. Stat. Mech.* 124004
[21] Proesmans K, Peliti L and Lacoste D 2018 (arXiv:1804.00859)
[22] Pietzonka P, Barato A C and Seifert U 2016 *Phys. Rev.* E **93** 052145
[23] Hwang W and Hyeon C 2018 *J. Phys. Chem. Lett.* **9** 513–20
[24] Wierenga H, ten Wolde P R and Becker N B 2018 *Phys. Rev.* E **97** 042404
[25] Brown A I and Sivak D A 2018 (arXiv:1805.08917)
[26] Pietzonka P and Seifert U 2018 *Phys. Rev. Lett.* **120** 190602
[27] Solon A P and Horowitz J M 2018 *Phys. Rev. Lett.* **120** 180605
[28] Vroylandt H, Lacoste D and Verley G 2018 *J. Stat. Mech.* 023205
[29] Nguyen M and Vaikuntanathan S 2016 *Proc. Natl Acad. Sci.* **113** 14231–6
[30] Lee S, Hyeon C and Jo J 2018 *Phys. Rev.* E **98** 032119
[31] Gingrich T R, Rotskoff G M and Horowitz J M 2017 *J. Phys. A: Math. Theor.* **50** 184004
[32] Li J, Horowitz J M, Gingrich T R and Fakhri N 2019 *Nat. Commun.* **10** 1666
[33] Ito S 2018 *Phys. Rev. Lett.* **121** 030605
[34] Hasegawa Y and Van Vu T 2018 (arXiv:1809.03292)
[35] Dechant A 2019 *EPL* **125** 20010
[36] Barato A C and Seifert U 2016 *Phys. Rev.* X **6** 041053
[37] Rotskoff G M 2017 *Phys. Rev.* E **95** 030101
[38] Proesmans K and Van den Broeck C 2017 *Europhys. Lett.* **119** 20001
[39] Ray S and Barato A C 2017 *J. Phys. A: Math. Theor.* **50** 355001
[40] Barato A C, Chetrite R, Faggionato A and Gabrielli D 2018 *New J. Phys.* **20** 103023
[41] Chiuchiù D and Pigolotti S 2018 *Phys. Rev.* E **97** 032109
[42] Barato A, Chetrite R, Faggionato A and Gabrielli D 2018 (arXiv:1810.11894)
[43] Koyuk T, Seifert U and Pietzonka P 2018 *J. Phys. A: Math. Theor.* **52** 02LT02
[44] Dechant A and Sasa S I 2018 *Phys. Rev.* E **97** 062101
[45] Holubec V and Ryabov A 2018 *Phys. Rev. Lett.* **121** 120601
[46] Macieszczak K, Brandner K and Garrahan J P 2018 *Phys. Rev. Lett.* **121** 130601
[47] Maes C 2017 *Phys. Rev. Lett.* **119** 160601
[48] Fischer L P, Pietzonka P and Seifert U 2018 *Phys. Rev.* E **97** 022143
[49] Van Vu T and Hasegawa Y 2019 (arXiv:1901.05715)
[50] Agarwalla B K and Segal D 2018 *Phys. Rev.* B **98** 155438
[51] Ptaszyński K 2018 *Phys. Rev.* B **98** 085425
[52] Carrega M, Sassetti M and Weiss U 2019 (arXiv:1901.10881)
[53] Brandner K, Hanazato T and Saito K 2018 *Phys. Rev. Lett.* **120** 090601
[54] Guarnieri G, Landi G, Clark S R and Goold J 2018 (arXiv:1901.10428)
[55] Spinney R E and Ford I J 2012 *Phys. Rev. Lett.* **108** 170603
[56] Deffner S and Saxena A 2015 *Phys. Rev. Lett.* **114** 150601
[57] Van den Broeck C and Toral R 2015 *Phys. Rev.* E **92** 012127
[58] Horowitz J M and Esposito M 2016 *Phys. Rev.* E **94** 020102
[59] Touchette H 2009 *Phys. Rep.* **478** 1–69
[60] Cover T M and Thomas J A 2012 *Elements of Information Theory* (New York: Wiley)
[61] Jarzynski C 2011 *Ann. Rev. Condens. Matter Phys.* **2** 329–51
[62] Feng E H and Crooks G E 2008 *Phys. Rev. Lett.* **101** 090602
[63] Crooks G E and Sivak D A 2011 *J. Stat. Mech.* P06003
[64] Granger L, Mehlis J, Roldán E, Ciliberto S and Kantz H 2015 *New J. Phys.* **17** 065005
[65] Crooks G E and Jarzynski C 2007 *Phys. Rev.* E **75** 021116
[66] Sivan U and Imry Y 1986 *Phys. Rev.* B **33** 551
[67] Butcher P 1990 *J. Phys.: Condens. Matter* **2** 4869
[68] Brandner K and Seifert U 2013 *New J. Phys.* **15** 105003
[69] Becker T, Willaert T, Cleuren B and Van den Broeck C 2015 *Phys. Rev.* E **91** 012101
[70] De Groot S R and Mazur P 2013 *Non-Equilibrium Thermodynamics* (New York: Dover Publications Inc.)

J. Stat. Mech. (2019) 054005